Preprints, 5th IFAC Conference on Nonlinear Model Predictive Control
September 17-20, 2015. Seville, Spain

Nonlinear MPC for Emission Efficient Cooperative Adaptive Cruise Control

Roman Schmied * **Harald Waschl** * **Rien Quirynen** **
Moritz Diehl ** **Luigi del Re** *

* *Institute for Design and Control of Mechatronical Systems, Johannes Kepler University Linz, Austria (e-mail: {roman.schmied, harald.waschl, luigi.delre}@jku.at)*
** *Department of Electrical Engineering, KU Leuven University, Belgium & Department IMTEK, University of Freiburg, Germany*

Abstract: Advanced driver assistant systems (ADAS) are primarily introduced to increase safety in every day traffic situations. Adaptive cruise control (ACC) systems represent an important example for such ADAS. The worldwide increasing traffic volume and the demand for the reduction of overall emissions call for the development of ADAS which concern not only safety but also the reduction of vehicle emissions and fuel consumption. In this work a cooperative adaptive cruise control (CACC) approach is introduced which focuses on these goals. A scenario with two consecutive driving vehicles and infrastructure-to-vehicle (I2V) communication is considered. The rear vehicle's longitudinal dynamics are controlled by a nonlinear model predictive control (NMPC) scheme with the target of emission and fuel efficient driving. The prospective velocity of the preceding vehicle is estimated by a prediction model based on the measured inter-vehicle distance and the I2V communication to enable an anticipatory driving behavior for the controlled vehicle. The results of hardware-in-the-loop (HIL) experiments on a dynamic engine test bench are presented and show a significant reduction of vehicle emissions and fuel consumption.

Keywords: Model Predictive Control, Intelligent Cruise Control, Automotive Emissions.

1. INTRODUCTION

Advanced driver assistant systems (ADAS) represent single parts of the puzzle on the way to autonomous driving. Supporting the driver in various every day traffic situations the interaction of ADAS to the vehicle varies from just giving advice or warnings, like the lane keeping assistant, up to taking over the whole vehicle control, as it is the case in parking assistance. Adaptive cruise control (ACC) systems represent a mixture, controlling longitudinal motion of the vehicle for general operation but leaving steering as well as emergency actions to the driver.

Such systems are nowadays available in production vehicles and implemented such that the vehicle automatically adapts its velocity according to a predecessor (if its velocity is lower than a setpoint) using a specific time-lag, see Xiao and Gao (2010) for a detailed review of the development of ACC systems. Several extensions and enhancements of ACC have been of high interest in academic and industrial research for the last years, mostly known under the name of cooperative adaptive cruise control (CACC). Thereby, communication either between vehicles (V2V) or between surrounding infrastructure and vehicles (I2V/V2I) is introduced to pursue different objectives.

Other approaches, Asadi and Vahidi (2011), Jones et al. (2014) aim to optimize trip duration and fuel consumption by introducing I2V communication between upcoming traffic lights and the controlled vehicle. Assuming that the driving route and the scheduling of traffic lights are known, traveling time and fuel consumption can be reduced using a receding horizon optimization strategy. However, it should be mentioned that within these works, influences of other traffic participants are neglected.

In the car following scenario considered in this paper the target of the controlled ego-vehicle is to reduce engine emissions and fuel consumption compared to its predecessor under the assumption of identical vehicles. This is achieved by introducing an admissible corridor for the inter-vehicle distance instead of using a specific time-gap value as it is the case in many ACC and CACC approaches. Within this corridor the ego-vehicle is free to move just pursuing the objective of increasing emission and fuel efficiency. Previous work using similar approaches for the inter-vehicle distance restriction focuses on fuel efficiency only and assumes that the velocity profile of the predecessor is known a priori, performing an offline optimization (Lang et al. (2013)) or a receding horizon strategy (Stanger and del Re (2013)).

However, typically the prospective behavior of other traffic participants is not known which makes an estimation of this external disturbance necessary. Some recent publications (Schmied et al. (2015b), Lang et al. (2014)) present data based heuristic prediction model approaches for the preceding driver's velocity and its effect on fuel efficiency. In Schmied et al. (2015c) a model predictive control (MPC) strategy is implemented and evaluated

Copyright © 2015 IFAC

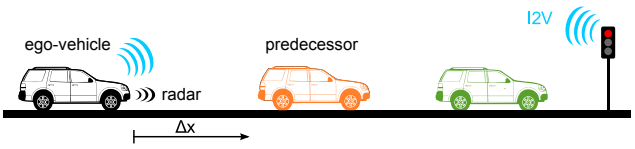


Fig. 1. CACC scenario considering I2V communication and measurement of the preceding vehicle.

experimentally with a test vehicle confirming results of previous simulations also on a real road. The approach in Moser et al. (2015a) uses stochastic modeling and MPC to account for prediction uncertainties within the control task. These approaches show high potential and possible further benefits in the reduction of fuel consumption.

In this paper a CACC scenario as illustrated in Fig. 1 is considered where the rear vehicle is referred to as the controlled ego-vehicle measuring relative distance and velocity of its predecessor with a radar sensor. Further, I2V communication is assumed to be available providing position and scheduling of upcoming traffic lights. A nonlinear model predictive control (NPMC) approach is applied to optimally control longitudinal dynamics of the ego-vehicle concerning engine emissions and fuel consumption.

Based on the information available from radar and I2V communication a prediction model is established to estimate the prospective velocity profile of the preceding vehicle. This enables an anticipatory driving behavior for the ego-vehicle which has been identified by previous research as crucial aspect for further increasing fuel efficiency . Prediction uncertainties are addressed indirectly within the cost function of the NMPC formulation. Simulation results are validated by performing hardware-in-the-loop (HIL) experiments on a dynamic engine test bench measuring engine emissions and fuel consumption precisely. The measurement results show a significant reduction of emissions and fuel consumption.

The paper first gives a general description of the problem including vehicle modeling and a background on engine emissions. Thereafter the structure and implementation of the NMPC as well as a disturbance prediction model to estimate the prospective velocity of the predecessor is described. Subsequently the paper presents the HIL measurement results and concludes with a summary and outlook.

2. GENERAL PROBLEM DESCRIPTION

Many ACC and CACC approaches rely on a specific value for the inter-vehicle distance Δx between the controlled ego-vehicle and its predecessor. Several spacing policies are discussed in literature, see e.g. Brackstone and McDonald (1999) for a historical review of car-following strategies. A widespread method is the implementation of a constant time headway policy for the desired inter-vehicle distance Δx_{des} given by

$$\Delta x_{des} = \Delta x_0 + t_h v \tag{1}$$

where Δx_0 denotes the desired distance at vehicle standstill, v the vehicle's velocity and t_h the constant time headway. However, all these approaches do not provide a degree of freedom to enable fuel and emission efficient

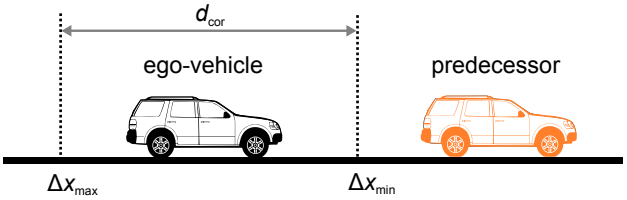


Fig. 2. Spacing policy with distance corridor for controlled vehicle

control since the desired inter-vehicle distance and hence the desired velocity are fixed.

Stanger and del Re (2013) addresses this drawback by introducing a distance corridor for the controlled ego-vehicle with boundaries $\Delta x_{\min}$ and $\Delta x_{\max}$ in which the vehicle is free to move. Fig. 2 depicts this strategy for the spacing policy. For the boundaries a constant time headway policy according to (1) is chosen

$$\Delta x_{\min} = \Delta x_0 + t_h v \tag{2a}$$
$$\Delta x_{\max} = \Delta x_{\min} + d_{cor} \tag{2b}$$

with a constant length d_{cor} for the corridor.

Hence, this spacing policy introduces a degree of freedom that allows the introduction of a control strategy for the ego-vehicle targeting reduction of fuel consumption and emissions compared to the predecessor.

2.1 Vehicle Modeling

The vehicle model is based on real world measurements performed with a production standard vehicle *BMW 320* with a Diesel engine and an 8-gear automatic gear box. The longitudinal vehicle dynamics for the considered car-following scenario can be approximated by a linear model in the form

$$\Delta\dot{x} = v_p - v \tag{3a}$$
$$\dot{v} = a \tag{3b}$$
$$\dot{a} = \frac{1}{\tau_v}(u - a) \tag{3c}$$

where x, v, a denote the position, velocity and acceleration of the vehicle, respectively, and u the input signal (gas and break pedal) normalized to the maximum acceleration. The velocity v_p of the predecessor is modeled as external disturbance. Fig. 3 shows the modeled and measured vehicle dynamics in form of a step response from input signal to acceleration to validate the linear approximation (3). Note that for illustration purposes all quantities are normalized to their maximum.

2.2 Diesel Engine Emissions

The control target for the CACC approach presented in this paper, namely reduction of emissions and fuel consumption, requires a basic understanding of the influence of the input signal (gas pedal) in this context. As for Diesel engines NOx and particulate matter (PM) emissions are most substantial, they are considered in this work. The reduction of emissions traditionally is a topic in the field of engine injection or airpath control, see e.g. Ferreau et al. (2007), Ortner and del Re (2007), Waschl et al.

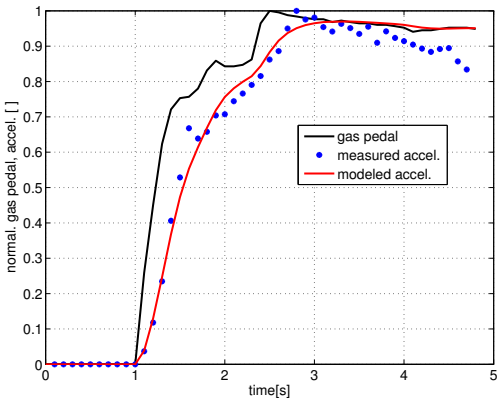


Fig. 3. Normed representation of step response from input signal to vehicle acceleration

(2012). Other works (Schmied et al. (2015a)) examine the influence of the injection system on engine emissions and represent the basis for the background on emissions covered in this section.

Different maneuvers for the gas pedal at constant engine speed were applied on a dynamic engine test bench equipped with a standard production 2l 4 cylinder Diesel engine which is equal to the one of the test-vehicle mentioned above. NOx and PM emissions are captured with a *Horiba 7100* and an *AVL Opacimeter*, respectively. Measurements reveal that both NOx and PM emissions show undesired peak values and an overshooting behavior for transient pedal maneuvers. Further, considering quasi stationary pedal profiles a disproportionate increase in NOx emissions could be observed.

These measurement results reveal that a reduction of engine emissions can be achieved by keeping the pedal input low and by avoiding fast transients. For the vehicle model as presented in (3) this means that changes in the input u and acceleration a should be kept small.

3. NONLINEAR MODEL PREDICTIVE CONTROL

Generally, anticipatory driving behavior means that based on the observation of different environmental influences the velocity v of the vehicle is adapted at a premature stage. The CACC approach considered in this paper accounts for those influences by measuring the inter-vehicle distance Δx and velocity v_p of the preceding vehicle with a radar sensor and by assuming that infrastructure-to-vehicle (I2V) communication is available for traffic lights providing their position x_{TL} and signal TL (red or green). This enables an estimation of the predecessor's prospective velocity $\hat{v}_p$ by introducing a prediction model. A nonlinear model predictive control (NMPC) strategy is introduced to achieve the objectives of emission and fuel efficient driving. Fig. 4 shows a block diagram of the control structure where the predecessor's velocity is treated as a disturbance.

To ensure safety of the controlled ego-vehicle the minimum inter-vehicle distance $\Delta x_{\min}$ in (2) must be kept strictly. Previous work using MPC strategies (Schmied et al. (2015c), Stanger and del Re (2013)) considered this restriction as constraint in the optimization problem. Near the minimum distance false estimation or unexpected

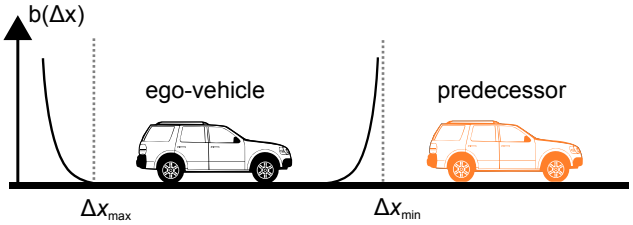


Fig. 5. Function $b(\Delta x)$ arising from constraints on the inter-vehicle distance Δx

behavior of the predecessor can easily lead to a constraint violation and hence to a threat of safety. The approach presented in Moser et al. (2015a) counteracts this issue by investigating a stochastic MPC explicitly considering estimation uncertainty. Exceeding the maximum distance $\Delta x_{\max}$ is generally not crucial but should be respected to maintain traffic flow and capacity. In this paper the restrictions for the distance corridor are considered directly in the cost function J of the optimal control problem using a barrier function for the minimum distance and a penalty function for the maximum distance

$$b(\Delta x) = \frac{c_1}{\Delta x - \Delta x_{\min}} + e^{\frac{\Delta x - \Delta x_{\max}}{c_2}} . \tag{4}$$

Hence, robustness against false estimation of the predecessor's velocity is provided and can be adjusted by the constants c_1 and c_2. Fig. 5 illustrates $b(\Delta x)$ arising from constraints on the inter-vehicle distance (4). To ensure feasibility of the NMPC, the measured inter-vehicle distance Δx is saturated to $\Delta x_{\min} + \epsilon$ with ϵ being a very small constant.

3.1 Optimal Control Formulation

Based on the results of section 2 and the distance policy (4) the following discretized optimal control problem (OCP) formulation can be obtained for receding horizon control using sample time T_s and horizon length N in the form

$$\min_{u_{k+i|k}} \sum_{i=0}^{N} \eta_1 a_{k+i|k}^2 + \eta_2 u_{k+i|k}^2 + \eta_3 b_{k+i|k}^2(\Delta\hat{x}) \tag{5a}$$

$$\begin{aligned} \text{s.t.} \quad z_{k+1|k} &= A z_{k|k} + b u_{k|k} \\ 0 &\le v_{k+i|k} \le v_{\max} \\ a_{\min} &\le a_{k+i|k} \le a_{\max} \qquad i = 0 \dots N \\ u_{\min} &\le u_{k+i|k} \le u_{\max} . \end{aligned} \tag{5b}$$

The notation $(\cdot)_{k+i|k}$ indicates the model based predicted quantities across the control horizon N at every sampling instant k. Note that the OCP objective (5a) is of nonlinear least squares type because of (4). Constraints to velocity v_k and acceleration a_k are indicated by the maximum torque and breaking power of the vehicle. The linear state equations in (5b) do not only include the vehicle model (3). For implementation purposes, to account for prospective values $\hat{v}_{p,k+i|k}$ of the measured disturbance $v_{p,k}$, they are considered in the state vector $z_k = [\Delta x_k \ \hat{v}_{p_0,k} \ \hat{v}_{p_1,k} \ \dots \ \hat{v}_{p_N,k} \ v_k \ a_k]^T$, too. Hence, the linear dynamics can be formulated as

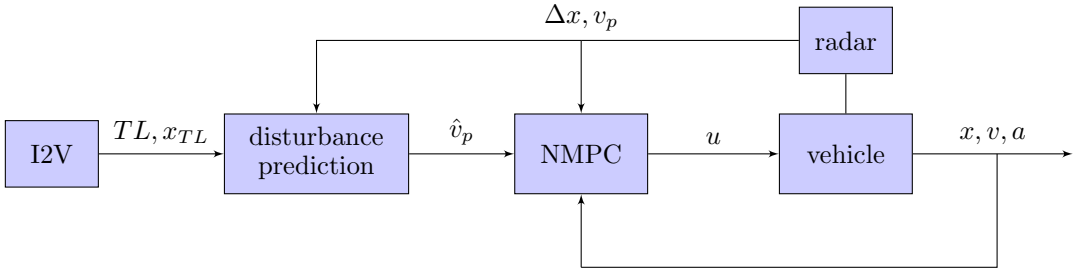


Fig. 4. Block diagram of control structure.

$$z_{k+1} = \begin{bmatrix} 1 & T_s & 0 & \dots & 0 & -T_s & 0 \\ 0 & 0 & 1 & 0 & \dots & 0 & 0 \\ \vdots & & & \ddots & & \vdots & \vdots \\ 0 & & \dots & & 1 & 0 & 0 \\ 0 & & \dots & & 1 & 0 & 0 \\ 0 & & \dots & & 0 & 1 & T_s \\ 0 & & \dots & & 1 & 0 & 1 - \frac{T_s}{\tau_v} \end{bmatrix} z_k + \begin{bmatrix} 0 & \dots & 0 & \frac{T_s}{\tau_v} \end{bmatrix}^T u_k \tag{6}$$

The ACADO Toolkit (Houska et al. (2011), Quirynen et al. (2013)) allows one to automatically generate efficient and real-time capable solvers based on the real-time iteration (RTI) scheme for NMPC. The code generation tool will be employed from MATLAB/SIMULINK to solve (5) in real-time using a sampling time of $T_s = 0.2s$.

3.2 Disturbance Prediction

In the CACC field of application the prediction of the predecessor's velocity v_p offers the possibility of anticipatory driving of the controlled ego-vehicle. Whereas some publications assume full knowledge of the predecessor's prospective velocity profile, Lang et al. (2014) investigates the influence of imperfect prediction approaches in the form of nonlinear ARX models on fuel efficiency of the ego-vehicle. In Moser et al. (2015b) a stochastic prediction strategy using Bayesian networks is presented. Thereby the identification is performed with real traffic measurements including traffic light signals.

Those measurement data constitute the basis for the prediction approach introduced in this paper, too. The distance to an upcoming traffic light is given by $d_{TL} = x_{TL} - x$ with x_{TL} and x denoting the position of the nearest upcoming traffic light and the position of the vehicle, respectively . It is assumed that I2V communication is limited to a maximum distance of $d_{TL_{\max}} = 200m$. Fig. 6 depicts a measured velocity profile and the corresponding distance d_{TL} and signal TL (red or green) of an upcoming traffic light.

The time delay τ_d between TL switching to green and a vehicle accelerating is dependent on the distance d_{TL} where the vehicle comes to a standstill because of a red traffic light signal. Fig. 7 illustrates measured values of the time delay τ_d against distance to traffic light d_{TL}. It can be observed that those measuring points can be approximated reasonably well by an affine function

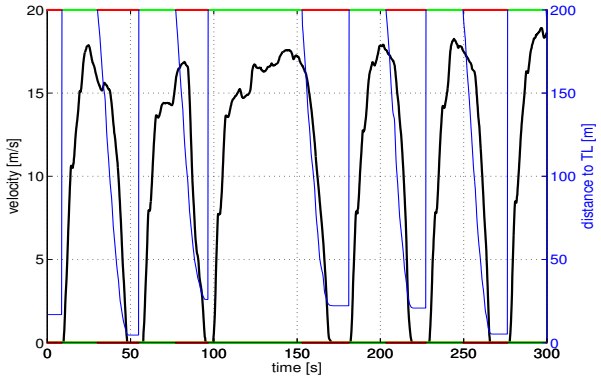


Fig. 6. Velocity profile v_p, distance d_{TL} and signal TL of traffic light (red or green) used for disturbance prediction

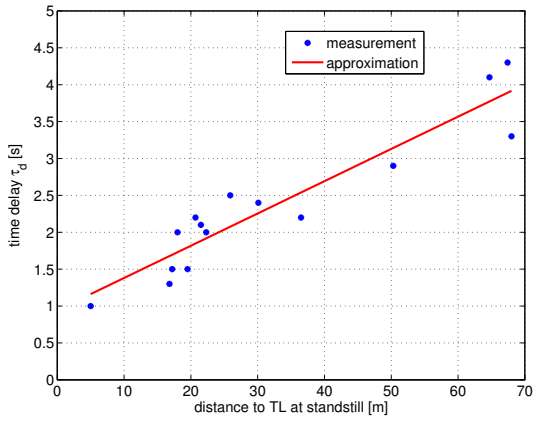


Fig. 7. Measured time delay τ_d as a function of the distance to the upcoming traffic light d_{TL}

$$\tau_d = p_0 + p_1 d_{TL} \tag{7}$$

with constant p_0, p_1.

Regarding the acceleration process of the vehicle after TL switches to green, denoted here with $\overline{TL}$ the velocity v_{accel} can be approximated using a first order transfer function where the gain is chosen according to the actual speed limit v_{lim}. At sampling instant k the remaining standstill instants $\zeta_{1,k}$ can be defined using the time delay (7) and the traffic light switching instant $\overline{TL}$

$$\zeta_{1,k} = \left(\overline{TL} + \frac{\tau_d}{T_s} - k \right) \sigma_{\overline{TL} + \frac{\tau_d}{T_s} - k} \,. \tag{8}$$

Here, σ_j denotes the Heaviside function which is used to account for the time delay τ_d. The velocity prediction for

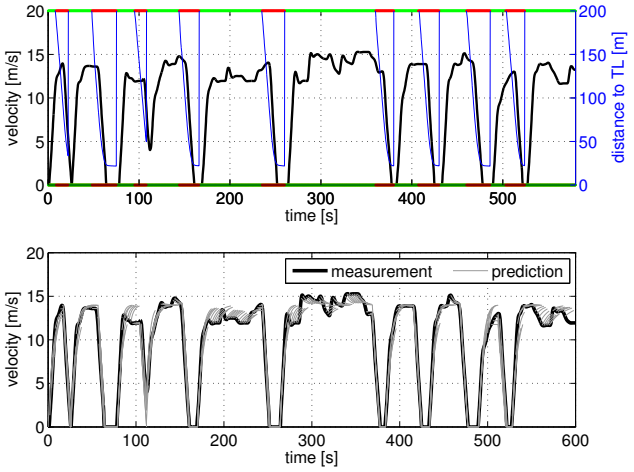


Fig. 8. Validation data and comparison of measured and predicted velocity profile $\hat{v}_{k+i|k}$ every 2 seconds

an acceleration maneuver due to a traffic light switching to green can therefore be described as

$$\hat{v}_{a,k+i|k} = (v_{lim} - v_k)\left(1 - e^{-\frac{(i-\zeta_{1,k})T_s}{\tau_a}}\right)\sigma_{i-\zeta_{1,k}} \qquad (9)$$
$$i = 0 \dots N\,.$$

Concerning the braking maneuver before an upcoming red traffic light it is supposed that the vehicle keeps the actual velocity v_k until a specific distance $d_{TL,b}$ to the traffic light. Generally, this distance is dependent on the traffic density but within this work assumed as constant. Equivalent to (8) at each sampling instant k a remaining delay

$$\zeta_{2,k} = \frac{d_{TL,k} - d_{TL,b}}{v_{p,k}T_s}\sigma_{d_{TL,k}-d_{TL,b}} \qquad (10)$$

can be introduced. The measurements in Fig. 6 reveal that after approaching $d_{TL,b}$ the vehicle brakes with nearly constant deceleration. The overall braking maneuver due to a red traffic light can therefore be described by

$$\hat{v}_{b,k+i|k} = v_{p,k} + \tilde{a}_{p,k}(i - \zeta_{2,k})\,T_s\sigma_{i-\zeta_{2,k}} \qquad (11)$$
$$i = 0 \dots N\,.$$

Using (9) and (11) the predicted velocity profile of the preceding vehicle can be formulated as

$$\hat{v}_{p,k+i|k} = \begin{cases} \hat{v}_{a,k+i|k} & TL_{k+i} = 1, i = 0 \dots N \\ \hat{v}_{b,k+i|k} & TL_{k+i} = 0, i = 0 \dots N\,. \end{cases} \qquad (12)$$

Fig. 8 depicts a comparison between measured and predicted velocity profiles where the validation data are shown in detail in the upper subplot. It can be observed that the disturbance prediction model (12) represents a very good approximation to the real measured data which is mainly due to the fact that traffic light signals are considered via I2V communication.

4. EXPERIMENTAL RESULTS

This section presents results obtained from hardware-in-the-loop (HIL) experiments on the dynamic test bench using the same measurement devices for NOx and PM emissions as mentioned in section 2. Additionally, a flow meter captures the injected fuel amount precisely. *AVL InMotion* is used for connecting a high fidelity vehicle

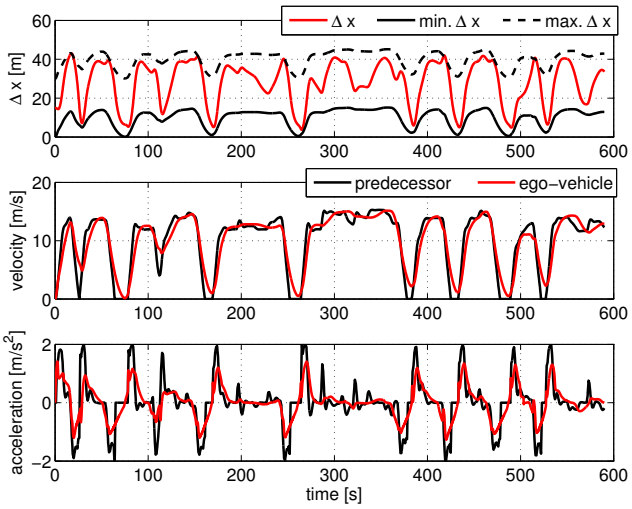


Fig. 9. Profiles for inter-vehicle distance Δx, velocities v, v_p and accelerations a, a_p of ego-vehicle and predecessor.

simulation environment to a real engine. The trajectory v_p for the preceding vehicle is selected according to the velocity profile depicted in Fig. 8. The parameters of the NMPC scheme are chosen to $\eta_1 = 20$, $\eta_2 = 50$, $\eta_3 = 20$, $\Delta x_0 = 0m$ and $d_{cor} = 30m$.

Fig. 9 depicts the results for the inter-vehicle distance Δx including the limits $\Delta x_{\min}$ and $\Delta x_{\max}$, and a comparison of the velocity and acceleration profiles v, v_p and a, a_p of the ego-vehicle and the predecessor. Thereby it can be clearly observed that the controlled ego-vehicle shows an anticipatory and smoothed driving behavior by using the disturbance prediction and the distance corridor.

Due to these prospective driving actions the fuel consumption and engine emissions can be reduced significantly compared to the preceding vehicle as presented in Fig. 10. The high values of PM emissions of the ego-vehicle at the beginning can be explained by the fact that medium or even low values of acceleration constitute adverse operating points of the engine. Nevertheless, the avoidance of high and sometimes unnecessary acceleration maneuvers leads to fuel and emissions efficient driving which can be concluded from table 1 showing the total values of fuel consumption, NOx and PM emissions.

Table 1. Results of HIL experiments regarding total emission and fuel consumption values.

	fuel cons.	NOx	PM
predecessor	263g	1	1
ego-vehicle	229g	0.76	0.72
Reduction	13%	24%	28%

Regarding computation time it should be mentioned that the OCP is solved within few milliseconds by the ACADO Toolkit which easily allowed for real-time implementation for the HIL experiments. Table 2 presents the minimum, maximum and mean computation time of NMPC iteration step.

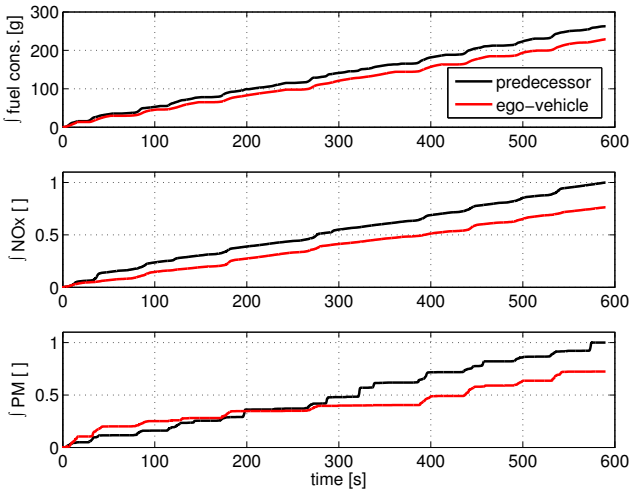


Fig. 10. Comparison of integrated fuel consumption and engine emissions NOx, PM from HIL measurements

Table 2. Minimum, maximum and mean computation time of a NMPC iteration.

Min	Max	Mean
23.23ms	26.44ms	23.47ms

5. CONCLUSIONS

The paper proposes an approach for fuel and emissions efficient cooperative adaptive cruise control using nonlinear model predictive control. A disturbance prediction model is introduced to estimate the prospective velocity profile of the preceding vehicle which consequently allows anticipatory driving behavior of the ego-vehicle with the proposed control strategy. Experimental results obtained by HIL measurements on a dynamic engine test bench show a significant reduction of vehicle emissions ans fuel consumption of the ego-vehicle compared to the predecessor whose trajectory is based on real world measurements.

Further work on this approach will cover more complex traffic situations handling more than one external traffic participant. Also, robustness of the controller against false estimation of the predecessor's behavior as well as variation of the predecessor due to e.g. lane change will be of great interest in further investigations.

ACKNOWLEDGEMENTS

This work has been partially supported by the Linz Center of Mechatronics (LCM) in the framework of the Austrian COMET-K2 program.

REFERENCES

Asadi, B. and Vahidi, A. (2011). Predictive Cruise Control: Utilizing Upcoming Traffic Signal Information for Improving Fuel Economy and Reducing Trip Time. *Control Systems Technology, IEEE Transactions on*, 19(3), 707–714.

Brackstone, M. and McDonald, M. (1999). Car-following: a historical review. *Transportation Research Part F: Traffic Psychology and Behaviour*, 2(4), 181 – 196.

Ferreau, H.J., Ortner, P., Langthaler, P., del Re, L., and Diehl, M. (2007). Predictive control of a real-world Diesel engine using an extended online active set strategy. *Annual Reviews in Control*, 31(2), 293 – 301.

Houska, B., Ferreau, H., and Diehl, M. (2011). ACADO Toolkit – An Open Source Framework for Automatic Control and Dynamic Optimization. *Optimal Control Applications and Methods*, 32(3), 298–312.

Jones, S., Huss, A., Kural, E., Massoner, A., Vock, C., and Tatschl, R. (2014). Development of Predictive Vehicle & Drivetrain Operating Strategies based upon Advanced Information & Communication Technologies (ICT). In *Transport Research Arena, Paris*.

Lang, D., Schmied, R., and del Re, L. (2014). Prediction of Preceding Driver Behavior for Fuel Efficient Cooperative Adaptive Cruise Control. *SAE Int. J. Engines*, 7(1), 14–20.

Lang, D., Stanger, T., and del Re, L. (2013). Opportunities on Fuel Economy Utilizing V2V Based Drive Systems. In *SAE Technical Paper 2013-01-0985*.

Moser, D., Waschl, H., Kirchsteiger, H., Schmied, R., and del Re, L. (2015a). Cooperative Adaptive Cruise Control Applying Stochastic Linear Model Predictive Control Strategies. In *to be published at European Control Conference (ECC) 2015*.

Moser, D., Waschl, H., Schmied, R., Efendic, H., and del Re, L. (2015b). Short Term Prediction of the Surrounding Traffic Velocity Using Bayesian Networks. In *to be published at SAE World Congress 2015*.

Ortner, P. and del Re, L. (2007). Predictive Control of a Diesel Engine Air Path. *Control Systems Technology, IEEE Transactions on*, 15(3), 449–456. doi: 10.1109/TCST.2007.894638.

Quirynen, R., Gros, S., and Diehl, M. (2013). Efficient NMPC for nonlinear models with linear subsystems. In *Decision and Control (CDC), 2013 IEEE 52nd Annual Conference on*, 5101–5106.

Schmied, R., Stadlbauer, S., Waschl, H., and del Re, L. (2015a). Improving the transient emission performance of a Diesel engine by input shaping techniques. In *to be published at SICE Annual Conference 2015*.

Schmied, R., Waschl, H., and del Re, L. (2015b). A Simplified Fuel Efficient Predictive Cruise Control Approach. In *SAE Technical Paper 2015-01-0296, 2015,*.

Schmied, R., Waschl, H., and del Re, L. (2015c). Extension and Experimental Validation of Fuel Efficient Predictive Adaptive Cruise Control. In *American Control Conference (ACC), 2015*.

Stanger, T. and del Re, L. (2013). A model predictive Cooperative Adaptive Cruise Control approach. In *American Control Conference (ACC), 2013*, 1374–1379.

Waschl, H., Alberer, D., and del Re, L. (2012). Multi Reference Model Predictive EGR Valve Control for Diesel Engines. In *Proceedings of the IFAC Workshop on Engine and Powertrain Control, Simulation and Modeling*, volume 3, 474–481.

Xiao, L. and Gao, F. (2010). A comprehensive review of the development of adaptive cruise control systems. *Vehicle System Dynamics*, 48(10), 1167–1192.